

Research Article

Single-cell atlases reveal leaf cell-type-specific regulation of metal transporters in the hyperaccumulator *Sedum alfredii* under cadmium stress

Guo Yu ^{a,b}, Jingyu Xiang ^a, Jie Liu ^{a,*}, Xuehong Zhang ^a, Hua Lin ^a, Geoffrey I. Sunahara ^d, Hongwei Yu ^c, Pingping Jiang ^a, Huachun Lan ^b, Juhui Qu ^{b,c}

^a College of Environmental Science and Engineering, Guilin University of Technology, Guilin 541004, China

^b State Key Joint Laboratory of Environment Simulation and Pollution Control, School of Environment, Tsinghua University, Beijing 100084, China

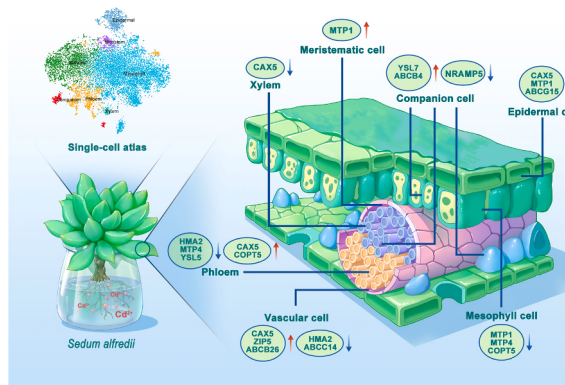
^c State Key Laboratory of Environmental Aquatic Chemistry, Research Center for Eco-Environmental Sciences, Chinese Academy of Sciences, Beijing 100085, China

^d Department of Natural Resource Sciences, McGill University, Montreal, Quebec, Canada

HIGHLIGHTS

- The first single-cell atlas for Cd hyperaccumulator *Sedum alfredii* was constructed.
- We provide a novel alternative approach to conduct scRNA-seq analysis for non-model plants.
- Metal transporters such as CAX5, COPT5, and ZIP5 were up-regulated in response to Cd stress in a cell-type-specific manner.

GRAPHICAL ABSTRACT



ARTICLE INFO

Keywords:
ScRNA-seq
Full-length transcriptome
Hyperaccumulator
Cd stress
Metal transporter

ABSTRACT

Hyperaccumulation in plants is a complex and dynamic biological process. *Sedum alfredii*, the most studied Cd hyperaccumulator, can accumulate up to 9000 mg kg⁻¹ Cd in its leaves without suffering toxicity. Although several studies have reported the molecular mechanisms of Cd hyperaccumulation, our understanding of the cell-type-specific transcriptional regulation induced by Cd remains limited. In this study, the first full-length transcriptome of *S. alfredii* was generated using the PacBio Iso-Seq technology. A total of 18,718,513 subreads (39.90 Gb) were obtained, with an average length of 2133 bp. The single-cell RNA sequencing was employed on leaves of *S. alfredii* grown under Cd stress. A total of 12,616 high-quality single cells were derived from the control and Cd-treatment samples of *S. alfredii* leaves. Based on cell heterogeneity and the expression profiles of previously reported marker genes, seven cell types with 12 transcriptionally distinct cell clusters were identified, thereby constructing the first single-cell atlas for *S. alfredii* leaves. Metal transporters such as CAX5, COPT5, ZIP5, YSL7, and MTP1 were up-regulated in different cell types of *S. alfredii* leaves under Cd stress. The distinctive gene expression patterns of metal transporters indicate special gene regulatory networks underlying Cd tolerance and

* Corresponding author.

E-mail address: liujie@glut.edu.cn (J. Liu).

hyperaccumulation in *S. alfredii*. Collectively, our findings are the first observation of the cellular and molecular responses of *S. alfredii* leaves under Cd stress and lay the cornerstone for future hyperaccumulator scRNA-seq investigations.

1. Introduction

Heavy metal contamination in soil, particularly cadmium (Cd), poses a widespread environmental threat to plant growth and human health [1]. In recent years, Cd contamination in arable soil has become a major concern which greatly decreases crop yield and threatens food safety [2]. Long-term exposure to Cd, even in minimal doses, can result in chronic health problems, including liver and kidney damage, which can progress to organ dysfunction and in extreme cases, organ failure [3]. Therefore, it is imperative to adopt effective approaches for the remediation of Cd-contaminated sites.

Phytoremediation emerges as a prospective technology for the remediation of Cd-contaminated soils, offering a sustainable and cost-effective alternative to conventional methods such as excavation, electrokinetics, and soil washing [4]. The efficacy of phytoremediation depends heavily on the employment of hyperaccumulators, which can accumulate high concentrations of heavy metals in the aerial tissues without suffering toxicity [5]. *Sedum alfredii* Hance, a plant from the *Crassulaceae* family native to China, is known as a zinc (Zn)/Cd co-hyperaccumulator and lead (Pb) accumulator [6–8]. This species can accumulate up to 9000 mg kg⁻¹ dry weight of Cd in its shoots without displaying significant toxicity symptoms [6], indicating the existence of a powerful defense mechanism that confers resilience against Cd toxicity [9].

Leaves serve as the main site for Cd accumulation in plants, where intricate mechanisms of metal detoxification and accumulation processes are involved [10]. Significant concentrations of Cd in *S. alfredii* can be found in the mesophyll cells of the leaves [11]. The mechanisms underlying Cd tolerance and hyperaccumulation in *S. alfredii* have been extensively studied by investigating its transcriptome, revealing a detoxification system that relies heavily on the expression of genes associated with metal transport [12,13]. However, conventional bulk transcriptome sequencing is limited to the characterization of genes responding to Cd stress at the whole-organ level, thereby obscuring the distinctive characteristics of different cell types [14]. Different tissues or cells demonstrate varying capabilities and functionalities in their response to Cd stress, which is mediated by distinct molecular mechanisms [15]. The varying strategies employed by different plant tissues of *S. alfredii* for adapting to Cd stress require further exploration.

Recent advances in single-cell RNA sequencing (scRNA-seq) technology have opened new avenues for a comprehensive elucidation of transcriptional regulatory landscapes and molecular differentiation trajectories across diverse cell types within complex multicellular tissues [16]. Several studies have recently applied scRNA-seq to understand cell-type heterogeneity and developmental trajectories in different plants, including *Arabidopsis* shoots and roots [17,18], *Zea mays* shoots and ears [19,20], *Oryza sativa* shoots and roots [21], *Arachis hypogaea* leaves [22], *Camellia sinensis* leaves [23], *Populus alba* stems [24], *Catharanthus roseus* leaves [25], *Glycine max* nodules [26], *Manihot esculenta* leaves and roots [27,28], *Phyllostachys edulis* roots [29], and *Triticum aestivum* roots [30]. In addition, some studies have elucidated the cell-type response of plant tissues under abiotic stress, including *Pisum sativum* under boron deficiency [31], *Arabidopsis* under phosphate deficiency [14], *Nicotiana tabacum* under nitrogen (N) deficiency [32], *Brassica rapa* ssp. *Pekinensis* under heat stress [33], *Gossypium arboreum* under salt stress [34], *Arabidopsis* under osmotic stress [35], and *Zea mays* under nitrate stress [36]. In general, the application of scRNA-seq remains limited to only a few plant species, due to the limited plant genomes reported. However, the response of hyperaccumulators such as *S. alfredii* to Cd stress at single-cell level needs further investigation.

In recent years, the field of plant scRNA-seq has made remarkable progress, as evidenced by a preponderance of investigations focusing on plants with known reference genomic sequences [37]. However, the transcriptional patterns of plants at the single-cell level with unknown genomes remain largely unexplored, thereby presenting a crucial gap in our understanding of plant biology [38]. Developing a universal approach for reconstructing scRNA-seq data in plants with unknown genomes would mark a substantial advancement for plant scRNA-seq studies.

In this study, third-generation full-length transcriptome sequencing was generated and used as an alternative to whole-genome sequencing for the hyperaccumulator *S. alfredii*. The first single-cell atlas for leaves of *S. alfredii* was constructed and the pathways and genes involved in Cd resistance based on cell lineage-specific expression patterns under Cd stress were elucidated. Notably, the cell-type-specific gene expression related to metal transport in plants was revealed for the first time. The present findings offer valuable insights into the Cd tolerance and hyperaccumulation mechanisms in plants at single-cell resolution.

2. Materials and methods

2.1. Plant growth and treatment

Seedlings of *S. alfredii* were collected from an old Pb/Zn mine in Zhejiang province, China. Healthy and uniform seedlings were chosen and cultivated in 25 % strength-modified Hoagland's nutrient solution for four weeks in a controlled greenhouse (12 h photoperiod, 25 °C day/20 °C night; light intensity, 200 μmol photons m⁻² s⁻¹; relative humidity, 65 %). The nutrient solution was constantly aerated and replaced every 3 d. The treated group consisted of pre-cultured seedlings exposed to 100 μM CdCl₂ for 24 h. The control group consisted of seedlings without exposure to additional heavy metals. The leaves were immediately frozen in liquid nitrogen for further analysis.

2.2. Full-length transcriptome sequence

RNA extraction was performed after tissue grinding in a Trizol reagent (Invitrogen, CA, USA), according to the manufacturer's guidelines. The Agilent 2100 Bioanalyzer and agarose gel electrophoresis were employed to evaluate the integrity of the extracted RNA. A Nanodrop micro-spectrophotometer from Thermo Fisher Scientific was used to determine the RNA's purity and concentration. The enrichment of mRNA was achieved using Oligo (dT) magnetic beads. PCR cycle optimization was employed to obtain the optimal amplification cycle count for subsequent PCR reactions. The BluePippinTM Size-Selection System (Sage Science, Beverly, MA, USA) was utilized for the size fractionation and selection (< 4 kb and > 4 kb). The SMRTbell template was paired followed by sequencing on the PacBio SequelII platform of Gene Denovo Biotechnology. The Pacific Biosciences (PacBio) Iso-Seq pipeline analyzed the raw sequencing data obtained from the cDNA libraries. The circular consensus sequence (CCS) which contained all the three structures of 5'primer, 3'primer, and poly(A) structures were designated as full-length sequences and were BLAST analyzed against the Nr, Swiss-Prot, KEGG, and KOG databases.

2.3. Protoplast isolation and scRNA-seq library construction

The leaf tips of *S. alfredii* seedlings from the control and Cd-treatment groups were cut into strips (1–2 mm) using sharp blades. These strips were quickly transferred to a filtered enzyme solution, which contained

0.5 % (w/v) pectinase, 8 % (w/v) mannitol (without Ca^{2+} and Mg^{2+}), 1.5 % (w/v) macerozyme R10, 1.5 % (w/v) cellulose R10, 10 mM CaCl_2 , 0.25 % (w/v) bovine serum albumin, 10 mM KCl, and 10 mM 2-morpholinoethanesulphonic acid. The mixture was shaken at 40 rpm for 2 h and filtered through a 40 μm cell strainer. The trypan blue staining method was used to assess the cell activity. The hemocytometer and microscope were employed to measure the cell concentration. The viability of cells in each sample > 95 %. Protoplasts were then suspended in 8 % (w/v) mannitol solution. Cells from all groups were mixed and diluted to 1000 cells/ μL . Sequencing libraries were constructed following the protocol provided by the manufacturer (10X Genomics) [39]. The barcoded sequencing libraries were assessed using an Agilent Bioanalyzer 2100. High-throughput sequencing of the libraries was conducted on an Illumina NovaSeq 6000 platform.

2.4. Raw data analysis

The Cell Ranger software (version 6.1.2) was used to obtain and process scRNA-seq raw data [40]. This involved mapping the sequencing reads to the full-length transcriptome of *S. alfredii* on the 10 \times Genomics platform. The Seurat R package (version 4.0.0) was employed for data quality control, cellular dimensionality reduction, and clustering. The DoubletFinder (v2.0.3) was used to remove GEMs with doublets. Cells with unusually high number of UMIs (≥ 8000) or mitochondrial gene percent ($\geq 10\%$) were filtered out. Cells with less than 500 or more than 4000 genes detected were also removed. Seurat R package facilitated the normalization and correction of raw data based on quality control metrics, thereby obtaining a set of highly variable genes.

2.5. Cell clustering and annotation

Principal component analysis (PCA) was conducted for feature selection. The t-distributed stochastic neighbor embedding (t-SNE) dimensionality reduction analysis was used for cell clustering and data. Seurat R was used to obtain differentially expressed genes (DEGs) and identified distinct marker genes of each cellular subgroup [41]. The DEGs were identified using the threshold of $P < 0.01$ and $\log_2 \text{FC} > 0.36$. The cell type was defined by analyzing reported marker genes and the correlations between the cell clusters. Novel marker genes were identified based on the criteria of $\log_2 \text{FC} > 0.5$ and $P < 0.01$, and the genes needed to be expressed in 25 % of cells of the target type. The expression patterns of these marker genes were illustrated using heatmaps and bubble plots.

2.6. Gene functional enrichment and pseudotime trajectory analyses

Gene ontology (GO) and Kyoto Encyclopedia of Genes and Genomes (KEGG) pathway enrichment analyses were conducted for the DEGs. The top 20 significantly enrichment pathways were used to generate an enrichment heatmap delineating the different cell types with the OmicShare platform (<https://www.omicshare.com/tools>).

Pseudotime trajectory analysis was conducted using Monocle (version 3.0), with a matrix of cells and their gene expression profiles [42]. Monocle facilitated the dimensionality reduction, condensing the data into a two-dimensional space while systematically ordering the cells ($\sigma = 0.001$, $\lambda = \text{NULL}$, $\text{param}.\gamma = 10$, $\text{tol} = 0.001$). Key genes associated with differentiation processes were identified with a false discovery rate (FDR) $< 1e^{-5}$. The genes exhibiting similar trends in expression were clustered. GO and KEGG enrichment analyses of the DEGs along the developmental trajectory were performed.

2.7. Weighted gene co-expression network analysis (WGCNA) within cell types

The relative relationships among genes with cell types of the control and Cd-treatment samples were obtained by the co-expression analysis

of the WGCNA package in R. The unsupervised hierarchical clustering approach was employed to generate a weighted adjacency matrix. The soft threshold power (β) was set at 14. We performed correlation analyses for specific traits or phenotypes. The Pearson correlations between each gene and their significance values were calculated. GO and KEGG pathway enrichment analyses were conducted for the genes in each module.

3. Results

3.1. Analysis of the full-length transcriptome sequence

The full-length transcriptome of *S. alfredii*, whose genome has not yet been published was sequenced (Fig. S1). After filtering the raw sequencing reads, 18,718,513 subreads were obtained, with an average length of 2133 bp and an N50 of 3222 bp. The total data volume of these subreads was equal to 39.90 Gb. Following the self-correction of all subreads, 605,443 circular consensus sequences were generated, which were subsequently utilized for the identification of full-length non-chimeric reads. The Cd-hit (version 4.6.7) tool was used to remove the redundant sequences. This process resulted in 37,395 transcripts having an average length of 1974 bp and an N50 of 2161 bp.

In total, 36,599 transcripts were successfully annotated in the Nr, KEGG, KOG, and Swiss-Prot databases (Table S1). Among these, 23,741 transcripts were found in all four databases. Specifically, the transcripts annotated by Nr, KEGG, KOG, and Swiss-Prot databases were 36,576 (99.94 %), 36,446 (99.64 %), 25,062 (68.48 %), and 31,665 (86.52 %), respectively (Fig. S2A). As shown in Fig. 2B, the largest number of homologous sequences were from *Vitis vinifera* (3775), *Nyssa sinensis* (2071), and *Camellia sinensis* (1143).

3.2. Generating the leaf cell atlas

Protoplasts from *S. alfredii* leaf tips were isolated to characterize the single-cell profiles. The cell number and viability were assessed by light microscopy (Fig. S3). More than 20,000 cells were labeled using the 10x Genomics platform. After thorough data filtering, a single-cell transcriptome of 12,616 high-quality protoplasts was obtained from the control and Cd-treatment samples. The median number of unique molecular identifiers (UMIs) per cell was 1570 in the control and 762 in the Cd-treatment samples. The median number of genes detected per cell was 831 in the control and 480 in the Cd-treatment samples. The scRNA-seq data obtained in this experiment were generally of high quality (Fig. 1A).

The scRNA-seq data were subjected to PCA dimensionality reduction and clustering analysis. There were 12 distinct cell clusters observed in both control and Cd-treatment samples (Fig. 1B; Fig. S4). The expression of several reported marker genes was compared across clusters to determine the cell types (Table S2). The mesophyll cells were marked by *FD1*, *PSAG*, *PSAL*, and *LHCA2* expressed in cluster 0, *ATPB*, *YCF4*, and *PSBB* expressed in cluster 4, *GRXS2* and *GRXC6* expressed in cluster 6, *PNC2*, *NPF6.4*, and *RPL34* expressed in cluster 8. The companion cells were marked by *SUC2*, *WRKY7*, *FER1*, and *AAP3* expressed in cluster 7, *SEOB*, *PXG4*, and *HVA22E* expressed in cluster 11. The epidermal cells were marked by *LTP10*, *CUT1*, *KCS11*, *KCS1*, and *FAR3* expressed in cluster 3. The vascular cells were marked by *BHLH66*, *NAC048*, *JAL2*, *ILL1*, and *LOX2.1* expressed in cluster 1. The phloem cells were marked by *AOC3*, *TIFY10A*, *GDH2*, and *BPS1* expressed in cluster 2, *TGG4*, *PAP26*, and *CYP83B1* expressed in cluster 10. The xylem cells were marked by *AT1G51060*, *HMGA*, *RPL23A*, and *AT2G30620* expressed in cluster 9. The meristem cells were marked by *CML11*, *RABB1C*, and *AT1G10030* expressed in cluster 5.

In summary, seven cell types were identified based on the expression patterns of the marker genes (Fig. 1C). They included mesophyll cells (7063 cells, clusters 0, 4, 6, and 8), companion cells (290 cells, clusters 7 and 11), epidermal cells (930 cells, cluster 3), vascular cells (2678 cells,

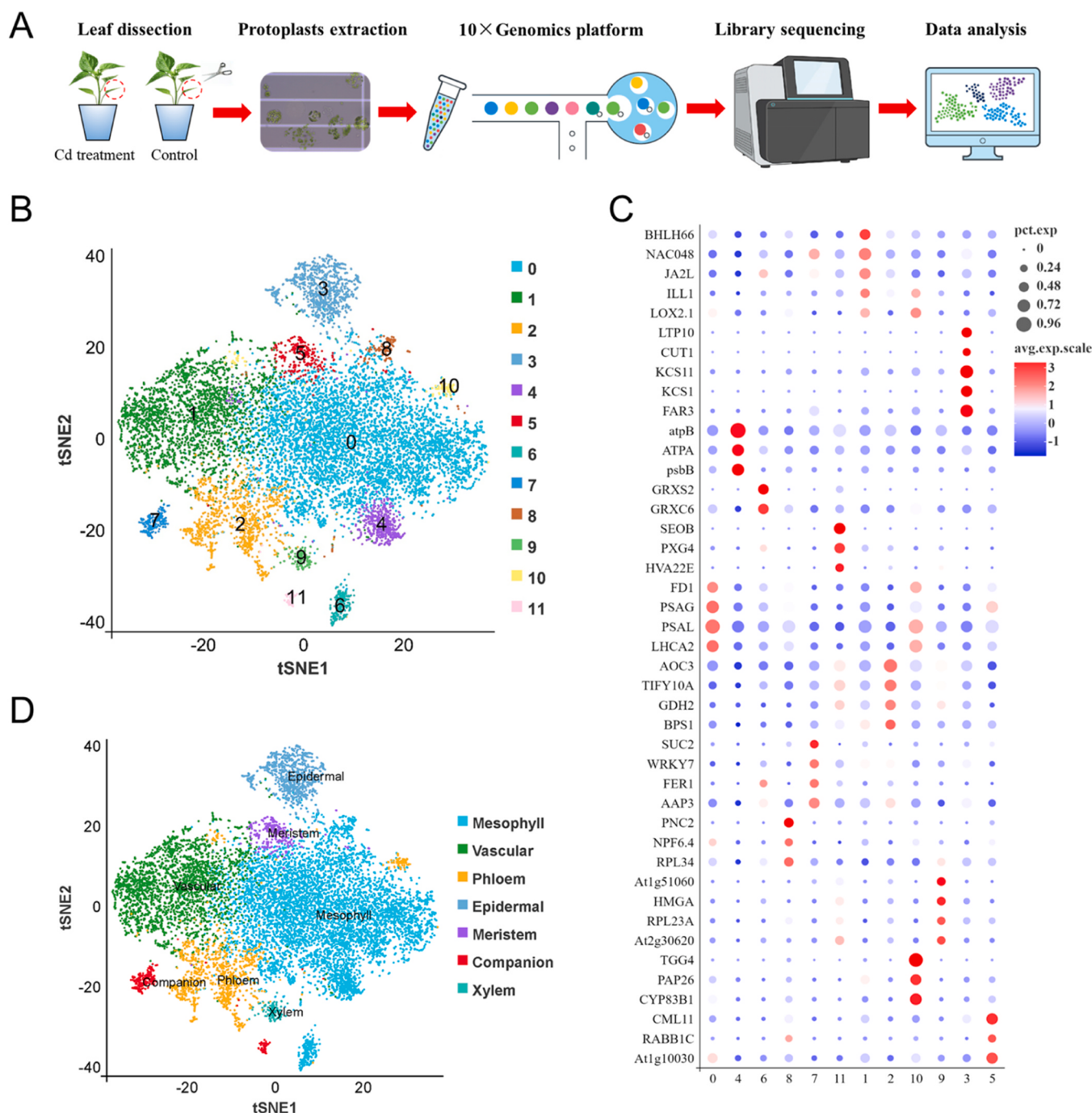


Fig. 1. Cell cluster analysis and annotation of cell types in *Sedum alfredii* leaves. (A) Protocol of single-cell library construction. (B) t-SNE visualization of the 12 clusters. (C) Expression patterns of 43 cell-type specific marker genes. (D) t-SNE visualization of the seven cell types based on marker gene analysis.

cluster 1), phloem cells (1203 cells, cluster 2 and 10), xylem cells (155 cells, cluster 9), and meristem cells (297 cells, cluster 5) (Fig. 1D and

Table 1
Number of cells in different cell types.

Cell type	Cell cluster	Number of cells	Percentage
Mesophyll cell	0, 4, 6, and 8	7063	55.98 %
Vascular cell	1	2678	21.23 %
Phloem	2 and 10	1203	9.54 %
Epidermal cell	3	930	7.37 %
Meristem cell	5	297	2.35 %
Companion cell	7 and 11	290	2.30 %
Xylem	9	155	1.23 %

Table 1).

GO and KEGG enrichment analyses were employed on the DEGs to validate the precision of cell type classification and investigate the molecular expression patterns of each cell type (Figs. S5 and S6; Tables S3 and S4). For example, DEGs in mesophyll cells were specifically enriched in photosynthesis-related biological processes. Epidermal cells were enriched for cutin, suberine, and wax biosynthesis, and fatty acid elongation processes. In phloem cells, DEGs were specifically enriched in alpha-linolenic acid metabolism processes.

3.3. Responses to Cd stress in a cell-type-specific manner

Both the control and Cd-treatment samples included the above seven

cell types and indicated that the cell classification was not affected by Cd stress (Fig. 2A). Compared to the control, Cd stress increased the proportion of phloem cells, xylem cells, and companion cells, whereas the proportion of mesophyll cells, vascular cells, and meristem cells was decreased. A total of 11,362 DEGs were identified in different cell types under Cd stress, including 1517 in mesophyll cells (405 up, 1112 down), 1520 in companion cells (461 up, 1059 down), 2298 in vascular cells (579 up, 1719 down), 2305 in epidermal cells (887 up, 1418 down), 2437 in phloem cells (988 up, 1449 down), 879 in xylem cells (360 up, 519 down), and 406 in meristem cells (265 up, 141 down) (Fig. S7; Table S5).

GO and KEGG pathway analyses were performed on the DEGs in each cell type responding to Cd stress (Fig. 2B; Tables S6 and S7). The GO

terms “photosynthesis,” “photosynthetic membrane,” and “photosystem” were enriched in DEGs of all cell types in the Cd-treatment sample relative to the control. In KEGG analysis, “photosynthesis” and “photosynthesis-antenna proteins” were enriched in DEGs of all cell types. Besides these two KEGG terms, the most enriched KEGG pathways were N metabolism and ribosome in companion cells, plant-pathogen interaction, glutathione (GSH) metabolism, and ribosome in epidermal cells, carbon fixation in photosynthetic organisms, N metabolism, GSH metabolism, ribosome, and phagosome in mesophyll cells, ribosome and phagosome in phloem cells, N metabolism and plant-pathogen interaction in vascular cells, ribosome in xylem cells.

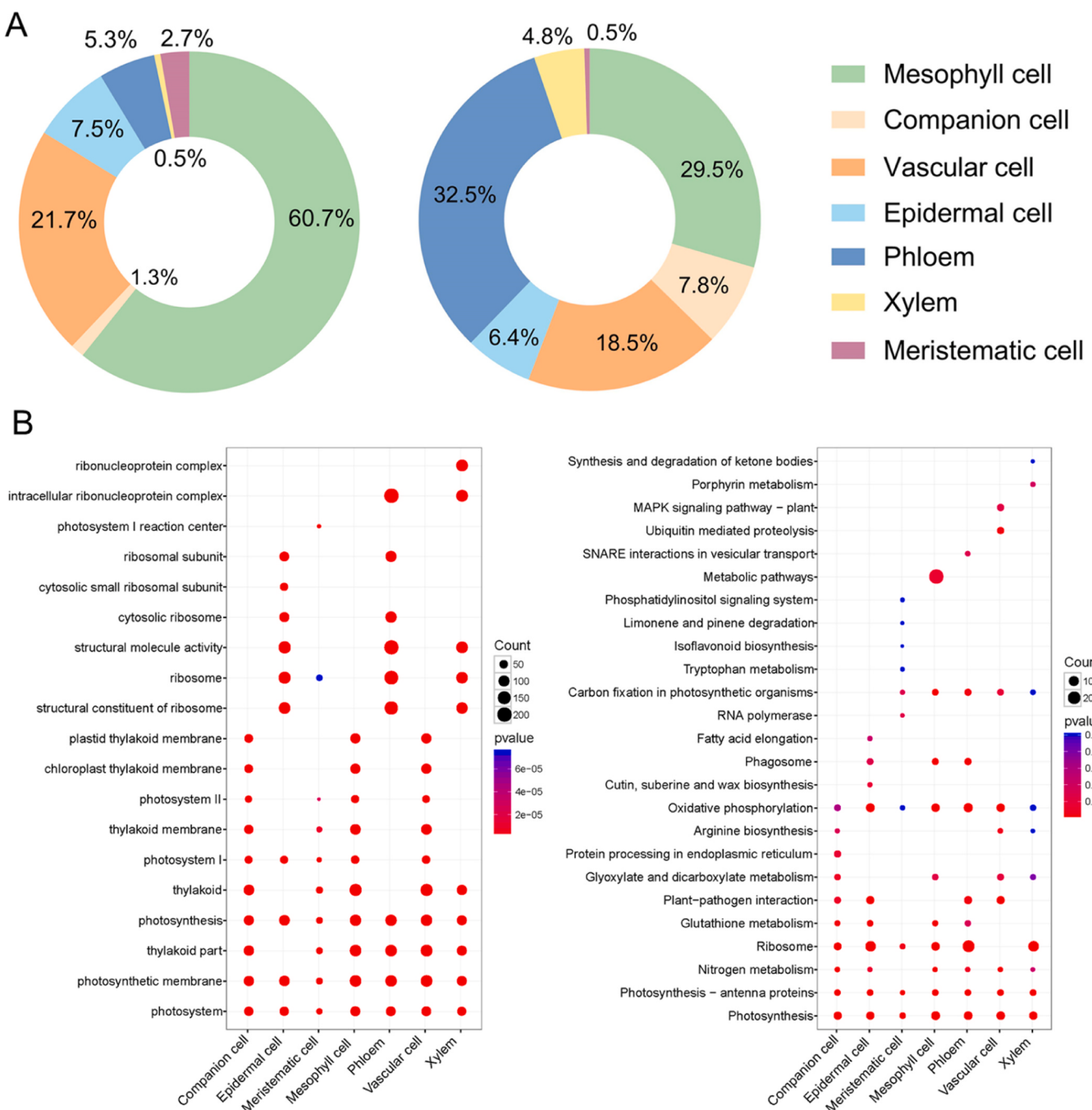


Fig. 2. Cell-type-specific responses to Cd stress. (A) The proportion of different cell types in the control (Left) and Cd treatment (Right) samples. (B) The most enriched GO (Left) and KEGG (Right) terms in differentially expressed genes of *Sedum alfredii* leaves in response to Cd stress in different cell types.

3.4. Cell-type-specific gene expression related to metal transport

The DEGs related to metal transport in response to Cd treatment were screened (Fig. 3; Table S5). Most of the genes related to metal transport exhibited cell type-specific expressions. For example, natural resistance-associated macrophage protein 5 (*NRAMP5*), ATP Binding Cassette Transporter B4 (*ABCB4*), and yellow stripe-like transporter 7 (*YSL7*) were mainly expressed in companion cells. *ABCG11*, *ABCB2*, and *ABCG15* were mostly expressed in epidermal cells. Heavy metal ATPase 2 (*HMA2*), *ABCB26*, and zinc/iron-regulated transporter 5 (*ZIP5*) were mainly expressed in vascular cells. Other genes were differentially expressed in more than one cell type. Metal tolerance protein 1 (*MTP1*) was expressed in the meristem, epidermal, and mesophyll cells. Cation exchanger 5 (*CAX5*) was expressed in xylem, vascular, and phloem cells.

3.5. Cell differentiation trajectory of mesophyll cells and xylem cells

Pseudotime analysis was performed on mesophyll cells and xylem cells to assess the impact of Cd stress on the developmental process of *S. alfredii* leaves (Fig. 4; Fig. S8). The gene expression matrices from the control and Cd-treatment samples were used to construct the differentiation trajectory. The pseudotime trajectory of mesophyll cells had seven different states (Fig. 4B). The cells shifted gradually from state 1 to state 7 as time progressed which represented the developmental process of mesophyll cells. Cd stress significantly decreased the proportion of cells in states 1, 3, and 6, indicating that Cd stress affected the differentiation progress of mesophyll cells (Fig. 4C). Additionally, the gene expression kinetics of the top 10 representative genes along the pseudotime progression were displayed, revealing that these genes were highly expressed in the late stage of cell development (Fig. S9). We selected the top 100 DEGs across the pseudotime order and these genes fell into seven clusters with distinct gene expression patterns (Fig. 4D; Table S8). For example, genes in cluster 1 were preferentially expressed at the end of the pseudotime trajectory. The KEGG terms related to plant-pathogen interaction, GSH metabolism, cutin, suberin, and wax biosynthesis were enriched at the beginning of the pseudotime. Photosynthesis, oxidative phosphorylation, ribosome, metabolic pathways, and RNA polymerase pathways were enriched at the end of the pseudotime.

3.6. Co-expression regulatory modules with key gene regulators in different cell types

The correlations between the key clusters and gene co-expression networks in response to Cd stress were constructed by the WGCNA package (Fig. S10). As a result, the co-expression network was composed of 13 distinct gene modules (Fig. S10B). Among the total of 32,875 DEGs identified, 8145 genes were found in the bisque3 module (Fig. 5A). Notably, the genes in the bisque3 module were mainly expressed in the xylem cells of the Cd-treatment sample compared to the lowly-expressed genes in the control (Fig. 5B). The KEGG pathways of ribosome, DNA replication, ribosome biogenesis in eukaryotes, and nucleocytoplasmic transport were significantly regulated in the bisque3 module (Fig. 5C). The genes in the antiquewhite1 module were mostly expressed in the mesophyll, xylem, and meristem cells of the control. The pathways of photosynthesis, photosynthesis-antenna proteins, carbon fixation in photosynthetic organisms, porphyrin metabolism, ribosome, and metabolic pathways were significantly regulated in the antiquewhite1 module (Fig. 5D).

4. Discussion

How do various types of plant cells contribute to organ structure and function? This question has long been perplexed by researchers in the field of plant science. The emergence of scRNA-seq technique has provided a powerful tool to investigate the heterogeneity within distinct cell populations at a single-cell resolution [43]. Despite its potential, there remain significant challenges in the plant scRNA-seq analysis. The successful isolation of individual plant cells from the tissue is essential for subsequent scRNA-seq analysis [44]. Although the enzymatic digestion-based isolation of protoplasts enables the removal of cell walls and the separation of individual cells, various factors such as cell wall composition, isolation techniques, and culture conditions can influence the efficiency of the isolation process [45]. For example, the negative effects of abiotic stress on plant cells could make it difficult to isolate high-quality protoplasts. Another challenge is the dependence of the current scRNA-seq analysis method on alignment with available reference genomes. Most economically important non-model plants do not have a reported genome sequence available [46]. The first full-length transcriptome of *S. alfredii* was generated here and used as a reference

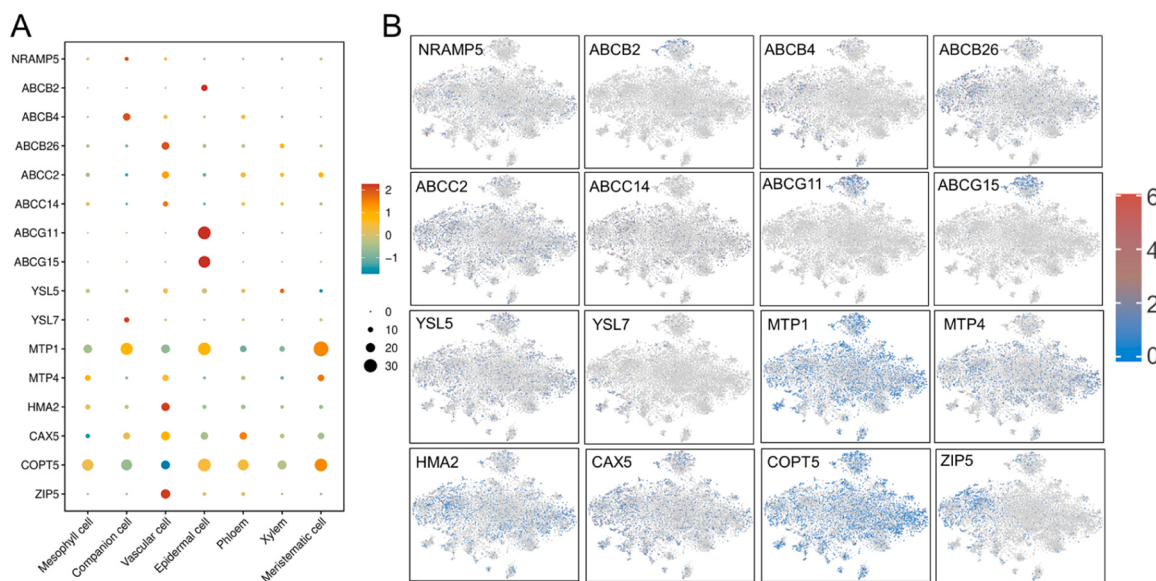


Fig. 3. Cell-type-specific gene expression patterns of DEGs related to metal transport. (A) The expression of metal transporters in different cell types. The dot diameter is the proportion of gene expressing within a specific cell cluster, and color represents the levels of their relative expression. (B) The cell distribution of metal transporters is shown by the t-SNE plot.

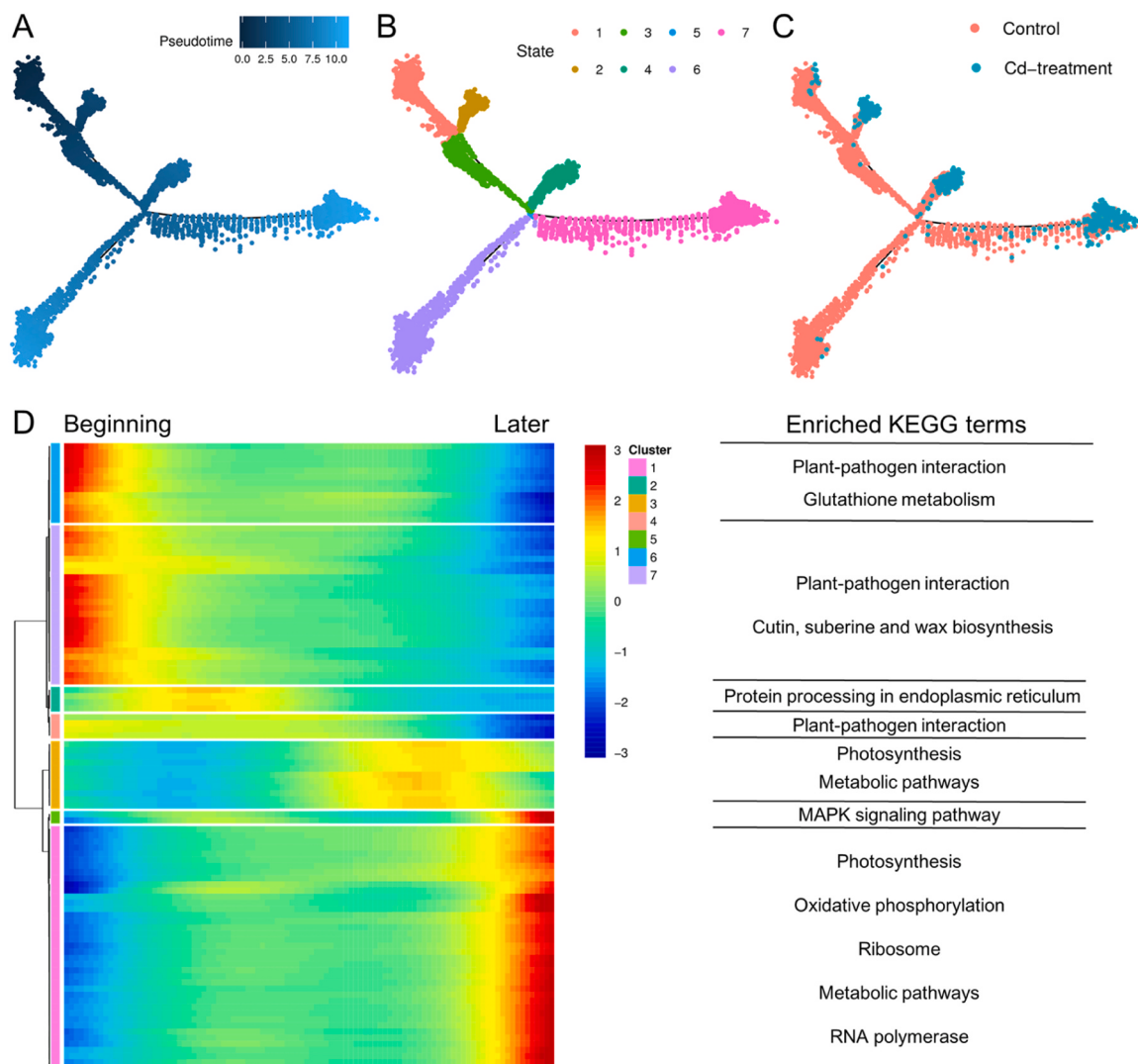


Fig. 4. Differentiation trajectory of mesophyll cells in the control and Cd-treatment samples. (A) Pseudotime trajectory from primordium to mesophyll cells. Each dot indicates an individual cell. Color shows the pseudo time score. (B) Distribution of cells in different states along the pseudotime trajectory. Colors represent different states. (C) Sample and cell cluster distributions along the pseudotime trajectory of mesophyll development. Colors indicate different samples. (D) Pseudotime heatmap of the top 100 DEGs. The bar color indicates the relative expression level of the genes. Representative KEGG metabolic pathways enriched in each population are highlighted.

for conducting the single-cell atlas of *S. alfredii* leaves in response to Cd stress.

The ability of hyperaccumulators to tolerate and accumulate heavy metals can be mediated by different metal transporters [47,48]. Cd is not an essential element for plants, so it is not surprising that plant systems do not possess a dedicated Cd transport pathway. Instead, Cd can be transported via other divalent ion channels such as Ca, Fe, or Zn channels [49]. A better understanding of the tolerance and accumulation strategy of Cd in plants is a prerequisite for the improvement of phytoremediation. In the present study, DEGs associated with metal transport in response to Cd treatment were screened and most of them exhibited cell type-specific expressions (Fig. 3). These DEGs belong to several metal transporter families such as NRAMP, ABC, YSL, MTP, HMA, CAX, COPT, and ZIP, whose functions have been reported in many plants including *S. alfredii* [50]. The ABC transporters exhibited significant enrichment in several cell types of *S. alfredii* leaves. The ABC transporters have been reported to be involved in Cd transport in plants [51]. In the present study, however, most DEGs from the ABC family were down-regulated in *S. alfredii* leaf cells. Considering the diverse functions of ABC transporters in the development and resistance

processes in plants, our findings indicate a potential involvement of ABC transporters through direct regulation of Cd translocation or participation in some indirect processes. Previous studies reported a significant interaction between Cd and Ca in *S. alfredii* in terms of translocation and distribution [52]. The CAX gene family plays an important role in maintaining intracellular Ca^{2+} homeostasis in plant cells [53]. The *SaCAX2h* identified in *S. alfredii* was involved in Ca and Mn accumulation and its overexpression in transgenic tobacco resulted in more Cd accumulation [54]. In our study, CAX5 was up-regulated in epidermal, vascular, and phloem cells, indicating that Ca^{2+} signaling may play key roles in Cd accumulation in these cell types. Some metal transporters are directly involved in Cd transport in plants. The ZIP transporters can transport a variety of divalent cations, including Zn^{2+} , Fe^{2+} , Mn^{2+} , and Cd^{2+} . The up-regulated ZIP in vascular cells of *S. alfredii* could play a significant role in Cd transport. Some members of the NRAMP gene family were involved in Cd transport in plants [55,56]. For instance, *SaNRAMP1* is crucial for the accumulation of Cd and Zn in *S. alfredii*, and the Cd, Mn, and Zn concentrations in the shoots of tobacco significantly increased when this gene was overexpressed [57]. NRAMP5 has been proved to restrict the movement of Cd from the cytoplasm to the xylem

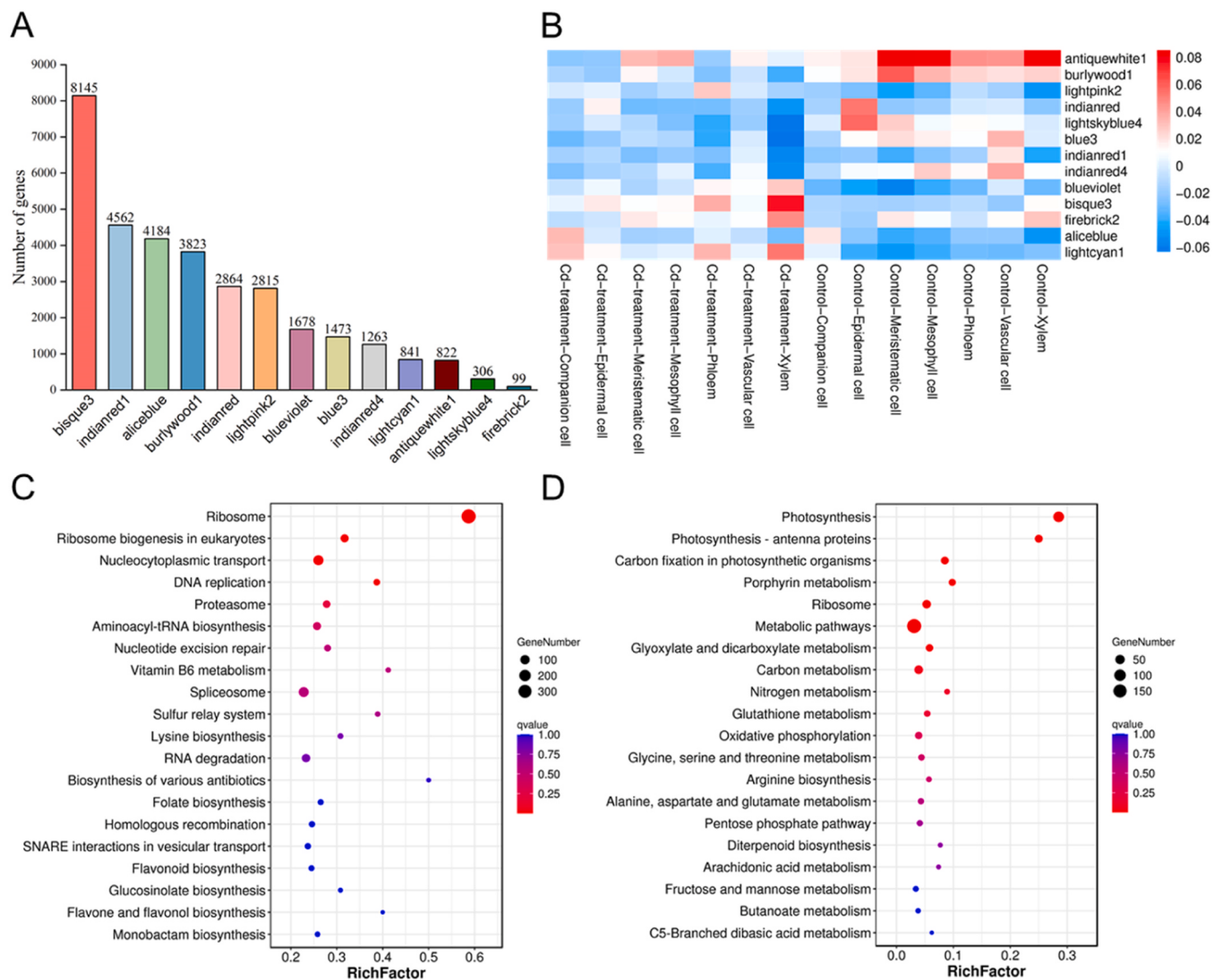


Fig. 5. Identification of key modules by weighted co-expression network. (A) The gene number in each module. (B) The gene expression patterns in different cell clusters of the control and Cd-treatment samples. (C) KEGG enrichment analysis of bisque3 module. (D) KEGG enrichment analysis of antiquewhite1 module.

[58]. In our study, NRAMP5 was down-regulated under Cd stress and mainly expressed in companion cells. The reason behind the down-regulation of NRAMP5 remains uncertain. Perhaps *S. alfredii* was coordinating the expression patterns of metal transporters in different leaf cells to facilitate the proper transport and storage of Cd. The MTP family is involved in Cd homeostasis and tolerance in plants [59]. Our results showed that MTP1 was up-regulated in meristematic cells, suggesting its potential roles in increasing transport efficiency and resistance to Cd. *S. alfredii* is a Cd hyperaccumulator and can maintain leaf growth under Cd stress [6]. The cell-type-specific difference in gene expression patterns of metal transporters reported here indicates that special strategies under Cd stress were developed. Based on the transcriptomic response of *S. alfredii* under Cd treatment at single-cell level, a gene regulatory working model is proposed (Fig. 6).

In summary, the expression of a handful of metal transporter families in the leaves of *S. alfredii* was differentially regulated in response to Cd stress. For instance, the intracellular and extracellular movement of Cd²⁺ was controlled by the expression dynamics of CAX5 in phloem, vascular, xylem, and epidermal cells, COPT5 in phloem, mesophyll cells. These transporters play a pivotal role in maintaining the intracellular ion equilibrium and transporting Cd²⁺ into vacuoles. The expression of NRAMP5 in companion cells may help restrict the movement of Cd²⁺ from the cytoplasm to the xylem. The expression of several ABC

transporter family in different cell types play a role in Cd-phytosiderophore transport and modulating the distribution of Cd²⁺.

5. Conclusion

Overall, a comprehensive single-cell transcriptome atlas was constructed here that enabled the analysis of leaf cell responses to Cd stress. To the best of our knowledge, this is the first report of a single-cell transcriptome in leaves of *S. alfredii*, a hyperaccumulator that has no reference genomes. Using the full-length transcriptome as a reference provides a reliable alternative for analyzing scRNA-seq data in *S. alfredii*. The responses of *S. alfredii* leaves to Cd stress showed highly heterogeneity, with different cell types exhibiting varying reactions that were closely related to their unique functions. Several metal transporter families such as CAX, COPT, and ZIP were differentially regulated in response to Cd stress in a cell-type-specific manner, indicating special gene regulatory networks underlying Cd tolerance and hyperaccumulation in *S. alfredii*. The genes characterized in this study can serve as targets for gene transfer and to conduct further genetic analyses for enhancing plant tolerance to heavy metal stress. This information enables researchers to precisely regulate gene expression and phenotypic changes within specific cell types or tissues.

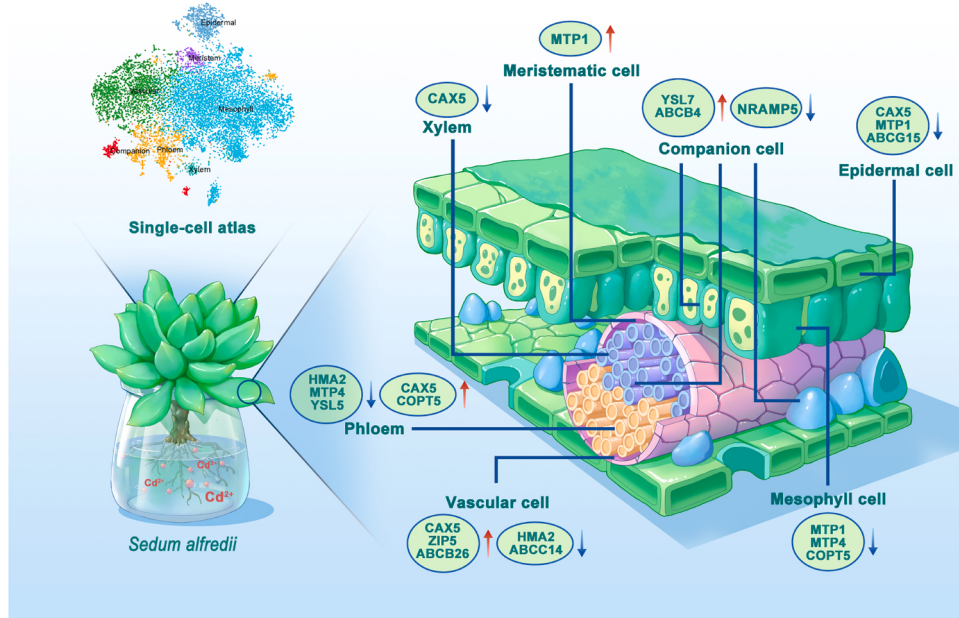


Fig. 6. Model of expression patterns of metal transporters at the cell-type level in response to Cd stress.

Environmental Implication

Understanding the cell-type-specific transcriptional regulation in response to heavy metal in hyperaccumulators is important for improving the efficiency of phytoremediation and is intriguing for evolutionary studies on plant adaption to abiotic stress. We constructed the first single-cell atlas for Cd hyperaccumulator *Sedum alfredii*. The distinctive gene regulatory networks of metal transporters were identified under Cd stress. These results provide valuable insights into the complex molecular mechanisms of Cd hyperaccumulation. They may help develop more efficient phytoremediation strategies to overcome environmental contamination.

CRediT authorship contribution statement

Hongwei Yu: Resources. **Geoffrey I. Sunahara:** Writing – review & editing. **Hua Lin:** Validation, Formal analysis. **Jiuhui Qu:** Writing – review & editing. **Huachun Lan:** Writing – review & editing. **Pingping Jiang:** Formal analysis. **Xuehong Zhang:** Supervision, Funding acquisition. **Jie Liu:** Writing – review & editing, Supervision, Project administration, Funding acquisition. **Jingyu Xiang:** Visualization, Methodology. **Guo Yu:** Writing – original draft, Visualization, Software, Methodology, Investigation, Conceptualization.

Declaration of Competing Interest

The authors declare that they have no known competing financial interests or personal relationships that could have appeared to influence the work reported in this paper.

Acknowledgments

This research was sponsored by the National Science Foundation of China (Grant No. 52200189, 52230006, 52225002, 52070051, 32271700, 52170154); Guangxi Bagui Youth Talent Support Program (GuiRenCaiBan [2024]30); the Guangxi Science and Technology Project (Grant No. 2021GXNSFBA220055, Guikeneng 2201Z001); Modern Industry College of Ecology and Environmental Protection, Guilin University of Technology.

Appendix A. Supporting information

Supplementary data associated with this article can be found in the online version at doi:10.1016/j.jhazmat.2024.136185.

Data Availability

Data will be made available on request.

References

- [1] Zhao, W.H., Ma, J., Liu, Q.Y., Qu, Y.J., Dou, L., Shi, H.D., Sun, Y., Chen, H.Y., Tian, Y.X., Wu, F.C., 2023. Accurate prediction of soil heavy metal pollution using an improved machine learning method: a case study in the Pearl River Delta, China. Environ Sci Technol 57 (46), 17751–17761.
- [2] Jing, H.N., Yang, W.T., Chen, Y.L., Yang, L.Y., Zhou, H., Yang, Y., Zhao, Z.J., Wu, P., Zia-Ur-Rehman, M., 2023. Exploring the mechanism of Cd uptake and translocation in rice: future perspectives of rice safety. Sci Total Environ 897, 165369.
- [3] Feng, S.D., Deng, S.X., Tang, Y., Liu, Y., Yang, Y., Xu, S.S., Tang, P., Lu, Y., Duan, Y., Wei, J., Liang, G.Y., Pu, Y.P., Chen, X., Shen, M.X., Yang, F., 2022. Microcystin-LR combined with cadmium exposures and the risk of chronic kidney disease: a case-control study in Central China. Environ Sci Technol 56 (22), 15818–15827.
- [4] Wei, Z.H., Le, Q.V., Peng, W.X., Yang, Y.F., Yang, H., Gu, H.P., Lam, S.S., Sonne, C., 2021. A review on phytoremediation of contaminants in air, water and soil. J Hazard Mater 403, 123658.
- [5] Yu, G., Jiang, P.P., Fu, X.F., Liu, J., Sunahara, G.I., Chen, Z., Xiao, H., Lin, F.Y., Wang, X.S., 2020. Phytoextraction of cadmium-contaminated soil by *Celosia argentea* Linn.: a long-term field study. Environ Poll 266, 115408. <https://doi.org/10.1016/j.envpol.2020.115408>.
- [6] Yang, X.E., Long, X.X., Ye, H.B., He, Z.L., Calvert, D.V., Stoffella, P.J., 2004. Cadmium tolerance and hyperaccumulation in a new Zn-hyperaccumulating plant species (*Sedum alfredii* Hance). Plant Soil 259 (1-2), 181–189.
- [7] Luo, J.P., Tao, Q., Jupa, R., Liu, Y.K., Wu, K., Song, Y.C., Li, J.X., Huang, Y., Zou, L., Y., Liang, Y.C., Li, T.Q., 2019. Role of vertical transmission of shoot endophytes in root-associated microbiome assembly and heavy metal hyperaccumulation in *Sedum alfredii*. Environ Sci Technol 53 (12), 6954–6963.
- [8] Hou, D., Wang, K., Liu, T., Wang, H.X., Lin, Z., Qian, J., Lu, L.L., Tian, S.K., 2017. Unique rhizosphere micro-characteristics facilitate phytoextraction of multiple metals in soil by the hyperaccumulating plant *Sedum alfredii*. Environ Sci Technol 51 (10), 5675–5684.
- [9] Li, J.T., Gurajala, H.K., Wu, L.H., A, E.N.T., Qiu, R.L., Baker, A.J.M., Tang, Y.T., Yang, X.E., Shu, W.S., 2018. Hyperaccumulator plants from China: a synthesis of the current state of knowledge. Environ Sci Technol 52 (21), 11980–11994.
- [10] Hu, Y., Tian, S.K., Foyer, C.H., Hou, D.D., Wang, H.X., Zhou, W.W., Liu, T., Ge, J., Lu, L.L., Lin, X.Y., 2019. Efficient phloem transport significantly remobilizes cadmium from old to young organs in a hyperaccumulator *Sedum alfredii*. J Hazard Mater 365, 421–429.
- [11] Tian, S.K., Lu, L.L., Labavitch, J., Yang, X.E., He, Z.L., Hu, H.N., Sarangi, R., Newville, M., Commissio, J., Brown, P., 2011. Cellular sequestration of cadmium in

- the hyperaccumulator plant species *Sedum alfredii*. *Plant Physiol* 157 (4), 1914–1925.
- [12] Ge, J., Tao, J.Y., Zhao, J.Q., Wu, Z.Y., Zhang, H.W., Gao, Y.X., Tian, S.K., Xie, R.H., Xu, S.Y., Liu, L.L., 2022. Transcriptome analysis reveals candidate genes involved in multiple heavy metal tolerance in hyperaccumulator *Sedum alfredii*. *Ecotox Environ Safe* 241, 112795.
- [13] Han, X., Yin, H., Song, X., Zhang, Y., Liu, M., Sang, J., Jiang, J., Li, J., Zhuo, R., 2016. Integration of small RNAs, degradome and transcriptome sequencing in hyperaccumulator *Sedum alfredii* uncovers a complex regulatory network and provides insights into cadmium phytoremediation. *Plant Biotechnol J* 14 (6), 1470–1483.
- [14] Wendrich, J.R., Yang, B.J., Vandamme, N., Verstaen, K., Smet, W., Van de Velde, C., Minne, M., Wybouw, B., Mor, E., Arents, H.E., Nolf, J., Van Duyse, J., Van Isterdael, G., Maere, S., Saeyns, Y., De Rybel, B., 2020. Vascular transcription factors guide plant epidermal responses to limiting phosphate conditions. *Science* 370 (6518), eaay4970.
- [15] Tian, S.K., Xie, R.H., Wang, H.X., Hu, Y., Hou, D.D., Liao, X.C., Brown, P.H., Yang, H.X., Lin, X.Y., Labavitch, J.M., Lu, L.L., 2017. Uptake, sequestration and tolerance of cadmium at cellular levels in the hyperaccumulator plant species *Sedum alfredii*. *J Exp Bot* 68 (9), 2387–2398.
- [16] Lafzi, A., Moutinho, C., Picelli, S., Heyn, H., 2018. Tutorial: guidelines for the experimental design of single-cell RNA sequencing studies. *Nat Protoc* 13 (12), 2742–2757.
- [17] Denyer, T., Ma, X.L., Klesen, S., Scacchi, E., Nieselt, K., Timmermans, M.C.P., 2019. Spatiotemporal developmental trajectories in the *Arabidopsis* root revealed using high-throughput single-cell RNA sequencing. *Dev Cell* 48 (6), 840–852.
- [18] Zhang, T.Q., Chen, Y., Wang, J.W., 2021. A single-cell analysis of the *Arabidopsis* vegetative shoot apex. *Dev Cell* 56 (7), 1056–1074.
- [19] Satterlee, J.W., Strable, J., Scanlon, M.J., 2020. Plant stem-cell organization and differentiation at single-cell resolution. *P Natl Acad Sci USA* 117 (52), 33689–33699.
- [20] Xu, X.S., Crow, M., Rice, B.R., Li, F., Harris, B., Liu, L., Demesa-Arevalo, E., Lu, Z.F., Wang, L.Y., Fox, N., Wang, X.F., Drenkow, J., Luo, A.D., Char, S.N., Yang, B., Sylvester, A.W., Gingeras, T.R., Schmitz, R.J., Ware, D., Lipka, A.E., Gillis, J., Jackson, D., 2021. Single-cell RNA sequencing of developing maize ears facilitates functional analysis and trait candidate gene discovery. *Dev Cell* 56 (4), 557–568.
- [21] Wang, Y., Huan, Q., Li, K., Qian, W.F., 2021. Single-cell transcriptome atlas of the leaf and root of rice seedlings. *J Genet Genom* 48 (10), 881–898.
- [22] Liu, H., Hu, D.X., Du, P.X., Wang, L.P., Liang, X.Q., Li, H., Lu, Q., Li, S.X., Liu, H.Y., Chen, X.P., Varshney, R.K., Hong, Y.B., 2021. Single-cell RNA-seq describes the transcriptome landscape and identifies critical transcription factors in the leaf blade of the allotetraploid peanut (*Arachis hypogaea* L.). *Plant Biotechnol J* 19 (11), 2261–2276.
- [23] Wang, Q., Wu, Y., Peng, A.Q., Cui, J.L., Zhao, M.Y., Pan, Y.T., Zhang, M.T., Tian, K., Schwab, W., Song, C.K., 2022. Single cell transcriptome atlas reveals developmental trajectories and a novel metabolic pathway of catechin esters in tea leaves. *Plant Biotechnol J* 20 (11), 2089–2106.
- [24] Chen, Y., Tong, S.F., Jiang, Y.Z., Ai, F.D., Feng, Y.L., Zhang, J.L., Gong, J., Qin, J.J., Zhang, Y.Y., Zhu, Y.Y., Liu, J.Q., 2021. Transcriptional landscape of highly lignified poplar stems at single-cell resolution. *Genome Biol* 22 (1), 319.
- [25] Sun, S.J., Shen, X.F., Li, Y., Li, Y., Wang, S., Li, R.C., Zhang, H.B., Shen, G.A., Guo, B.L., Wei, J.H., Xu, J., St-Pierre, B., Chen, S.L., Sun, C., 2023. Single-cell RNA sequencing provides a high-resolution roadmap for understanding the multicellular compartmentation of specialized metabolism. *Nat Plants* 9 (1), 179–190.
- [26] Sun, B.C., Wang, Y., Yang, Q., Gao, H., Niu, H.Y., Li, Y.S., Ma, Q., Huan, Q., Qian, W.F., Ren, B., 2023. A high-resolution transcriptomic atlas depicting nitrogen fixation and nodule development in soybean. *J Integr Plant Biol* 65 (6), 1536–1552.
- [27] Zang, Y.W., Pei, Y.C., Cong, X.L., Ran, F.F., Liu, L.W., Wang, C.Y., Wang, D.Y., Min, Y., 2024. Single-cell RNA-sequencing profiles reveal the developmental landscape of the *Manihot esculenta* Crantz leaves. *Plant Physiol* 104 (1), 456–474.
- [28] Song, J.J., Fan, B.J., Shao, X.D., Zang, Y.W., Wang, D.Y., Min, Y., 2023. Single-cell transcriptome sequencing atlas of cassava tuberous root. *Front Plant Sci* 13, 1053669.
- [29] Cheng, Z.C., Mu, C.H., Li, X.Y., Cheng, W.L., Cai, M.M., Wu, C.Y., Jiang, J.T., Fang, H., Bai, Y.C., Zheng, H.F., Geng, R.M., Xu, J.L., Xie, Y.L., Dou, Y.P., Li, J., Mu, S.H., Gao, J., 2023. Single-cell transcriptome atlas reveals spatiotemporal developmental trajectories in the basal roots of moso bamboo (*Phyllostachys edulis*). *Hortic Res* 10 (8), uhad122.
- [30] Zhang, L.H., He, C., Lai, Y.T., Wang, Y.T., Kang, L., Liu, A.K., Lan, C.X., Su, H.D., Gao, Y.W., Li, Z.Q., Yang, F., Li, Q., Mao, H.L., Chen, D.J., Chen, W., Kaufmann, K., Yan, W.H., 2023. Asymmetric gene expression and cell-type-specific regulatory networks in the root of bread wheat revealed by single-cell multiomics analysis. *Genome Biol* 24 (1), 65.
- [31] Chen, X., Ru, Y.Q., Takahashi, H., Nakazono, M., Shabala, S., Smith, S.M., Yu, M., 2023. Single-cell transcriptomic analysis of pea shoot development and cell-type-specific responses to boron deficiency. *Plant J* 117 (1), 302–322.
- [32] Feng, Y.Q., Zhao, Y.Y., Ma, Y.J., Liu, D.S., Shi, H.Z., 2023. Single-cell transcriptome analyses reveal cellular and molecular responses to low nitrogen in burley tobacco leaves. *Physiol Plant* 175 (6).
- [33] Sun, X.X., Feng, D.L., Liu, M.Y., Qin, R.X., Li, Y., Zhang, X.M., Wang, Y.H., Shen, S.X., Ma, W., Zhao, J.J., 2022. Single-cell transcriptome reveals dominant subgenome expression and transcriptional response to heat stress in Chinese cabbage. *Genome Biol* 23 (1), 262.
- [34] Li, P.T., Liu, Q.K., Wei, Y.Y., Xing, C.Z., Xu, Z.P., Ding, F., Liu, Y.L., Lu, Q.W., Hu, N., Wang, T., Zhu, X.Q., Cheng, S., Li, Z.G., Zhao, Z.L., Li, Y.F., Han, J.P., Cai, X.Y., Zhou, Z.L., Wang, K.B., Zhang, B.H., Liu, F., Jin, S.X., Peng, R.H., 2024. Transcriptional landscape of cotton roots in response to salt stress at single-cell resolution. *Plant Commun* 5 (2), 100740.
- [35] Liu, Q., Ma, W., Chen, R.Y., Li, S.T., Wang, Q.F., Wei, C., Hong, Y.J., Sun, H.X., Cheng, Q., Zhao, J.J., Kang, J.M., 2024. Multiome in the same cell reveals the impact of osmotic stress on *Arabidopsis* root tip development at single-cell level. *Adv Sci* 11 (24).
- [36] Li, X.H., Zhang, X.B., Gao, S., Cui, F.Q., Chen, W.W., Fan, L.N., Qi, Y.W., 2022. Single-cell RNA sequencing reveals the landscape of maize root tips and assists in identification of cell type-specific nitrate-response genes. *Crop J* 10 (6), 1589–1600.
- [37] Bawa, G., Liu, Z.X., Yu, X.L., Tran, L.S.P., Sun, X.W., 2024. Introducing single cell stereo-sequencing technology to transform the plant transcriptome landscape. *Trends Plant Sci* 29 (2), 249–265.
- [38] Yu, X.L., Liu, Z.X., Sun, X.W., 2023. Single-cell and spatial multi-omics in the plant sciences: technical advances, applications, and perspectives. *Plant Commun* 4 (3), 100508.
- [39] Zhang, T., Xu, Z., Shang, G., Wang, J., 2019. A single-cell RNA sequencing profiles the developmental landscape of *Arabidopsis* root. *Mol Plant* 12, 648–660.
- [40] Stuart, T., Butler, A., Hoffman, P., Hafemeister, C., Papalexi, E., Mauck, W.M., Hao, Y., Stoeckius, M., Smibert, P., Satija, R., 2019. Comprehensive integration of single-cell data. *Cell* 177, 1888–1902.e21.
- [41] Cao, J., Spielmann, M., Qiu, X., Huang, X., Ibrahim, D.M., Hill, A.J., Zhang, F., Mundlos, S., Christiansen, L., Steemers, F.J., Trapnell, C., Shendure, J., 2019. The single-cell transcriptional landscape of mammalian organogenesis. *Nature* 566, 496–502.
- [42] Qiu, X.J., Mao, Q., Tang, Y., Wang, L., Chawla, R., Pliner, H.A., Trapnell, C., 2017. Reversed graph embedding resolves complex single-cell trajectories. *Nat Methods* 14 (10), 979–982.
- [43] Kaur, H., Jha, P., Ochatt, S.J., Kumar, V., 2024. Single-cell transcriptomics is revolutionizing the improvement of plant biotechnology research: recent advances and future opportunities. *Crit Rev Biotechnol* 44 (2), 202–217.
- [44] Oliva, M., Lister, R., 2023. Exploring the identity of individual plant cells in space and time. *N Phytol* 240 (1), 61–67.
- [45] Shaw, R., Tian, X., Xu, J., 2021. Single-cell transcriptome analysis in plants: advances and challenges. *Mol Plant* 14 (1), 115–126.
- [46] Ali, M., Yang, T.X., He, H., Zhang, Y., 2024. Plant biotechnology research with single-cell transcriptome: recent advancements and prospects. *Plant Cell Rep* 43 (3), 75.
- [47] Yang, Z., Yang, F., Liu, J.L., Wu, H.T., Yang, H., Shi, Y., Liu, J., Zhang, Y.F., Luo, Y.R., Chen, K.M., 2022. Heavy metal transporters: functional mechanisms, regulation, and application in phytoremediation. *Sci Total Environ* 809, 109408.
- [48] Yu, G., Ullah, H., Wang, X.S., Liu, J., Chen, B.L., Jiang, P.P., Lin, H., Geoffrey, S., You, S.H., Zhang, X.H., Shahab, A., 2023. Integrated transcriptome and metabolome analysis reveals the mechanism of tolerance to manganese and cadmium toxicity in the Mn/Cd hyperaccumulator *Celosia argentea* Linn. *J Hazard Mater* 443, 130206.
- [49] Han, M., Ullah, H., Yang, H., Yu, G., You, S., Liu, J., Chen, B., Shahab, A., Antoniadis, V., Shaheen, S.M., Rinklebe, J., 2023. Cadmium uptake and membrane transport in roots of hyperaccumulator *Amaranthus hypochondriacus* L. *Environ Pollut* 331 (1), 121846.
- [50] Chen, X.Q., Zhao, Y.C., Zhong, Y.Q., Chen, J.J., Qi, X., 2023. Deciphering the functional roles of transporter proteins in subcellular metal transportation of plants. *Planta* 258 (1), 17.
- [51] Yang, G.Z., Fu, S., Huang, J.J., Li, L.Y., Long, Y., Wei, Q.X., Wang, Z.G., Chen, Z., Xia, J., 2021. The tonoplast-localized transporter OsABCC9 is involved in cadmium tolerance and accumulation in rice. *Plant Sci* 307, 110894.
- [52] Liu, Y.K., Tao, Q., Guo, X.Y., Luo, J.P., Li, J., Liang, Y., Li, T.Q., 2020. Low calcium-induced delay in development of root apoplastic barriers enhances Cd uptake and accumulation in *Sedum alfredii*. *Sci Total Environ* 723, 137810.
- [53] He, F., Shi, Y.J., Li, J.L., Lin, T.T., Zhao, K.J., Chen, L.H., Mi, J.X., Zhang, F., Zhong, Y., Lu, M.M., Niu, M.X., Feng, C.H., Ding, S.S., Peng, M.Y., Huang, J.L., Yang, H.B., Wan, X.Q., 2022. Genome-wide analysis and expression profiling of Cation/H⁺ exchanger (CAX) family genes reveal likely functions in cadmium stress responses in poplar. *Int J Biol Macromol* 204, 76–88.
- [54] Zhang, M., Zhang, J., Lu, L.L., Zhu, Z.Q., Yang, X.E., 2016. Functional analysis of CAX2-like transporters isolated from two ecotypes of *Sedum alfredii*. *Biol Plant* 60 (1), 37–47.
- [55] Sasaki, A., Yamaji, N., Yokoshio, K., Ma, J.F., 2012. *Nramp5* is a major transporter responsible for manganese and cadmium uptake in rice. *Plant Cell* 24 (5), 2155–2167.
- [56] Zhang, J.S., Zhang, X.L., Jia, M.G., Fu, Q., Guo, Y.S., Wang, Z.H., Kong, D.J., Lin, Y.C., Zhao, D.G., 2023. Two novel transporters *NtNRAMP6a* and *NtNRAMP6b* are involved in cadmium transport in tobacco (*Nicotiana tabacum* L.). *Plant Physiol Bioch* 202, 107953.
- [57] Zhang, J., Zhang, M., Shohag, M.J.I., Tian, S.K., Song, H.Y., Feng, Y., Yang, X., 2016. Enhanced expression of *SahMA3* plays critical roles in Cd hyperaccumulation and hypertolerance in Cd hyperaccumulator *Sedum alfredii* Hance. *Planta* 243 (3), 577–589.
- [58] Chang, J.D., Huang, S., Konishi, N., Wang, P., Chen, J., Huang, X.Y., Ma, J.F., Zhao, F.J., 2020. Overexpression of the manganese/cadmium transporter *OsNRAMP5* reduces cadmium accumulation in rice grain. *J Exp Bot* 71, 5705–5715.
- [59] Das, N., Bhattacharya, S., Maiti, M.K., 2016. Enhanced cadmium accumulation and tolerance in transgenic tobacco overexpressing rice metal tolerance protein gene *OsMTP1* is promising for phytoremediation. *Plant Physiol Bioch* 105, 297–309.